Supplemental Information

Homogenizing SAMs deposition via seeding -OH groups for scalable fabrication of perovskite solar cells

Sheng Fu,*[a+] Nannan Sun,[a+] Hao Chen,[b] You Li,[b] Yunfei Li,[a] Xiaotian Zhu,[a] Bo Feng,[a] Xueming Guo,[a] Canglang Yao,[c] Wenxiao Zhang,[a] Xiaodong Li*[a] and Junfeng Fang*[a]

[a.] School of Physics and Electronic Science, Engineering Research Center of Nano-photonics and Advanced Instrument Ministry of Education, East China Normal University, Shanghai 200062, China.
Email: sfu@phy.ecnu.edu.cn; xdli@phy.ecnu.edu.cn; jffang@phy.ecnu.edu.cn

[b.] Global Institute of Future Technology (GIFT), Shanghai Jiao Tong University, Shanghai 200240, China

[c.] Laboratory of Advanced Materials, Fudan University, Shanghai 200438, China

[+]These authors contribute equally to this work.

*Corresponding Authors: sfu@phy.ecnu.edu.cn; xdli@phy.ecnu.edu.cn; jffang@phy.ecnu.edu.cn

Experimental Part

Materials and solution preparations

The materials for perovskite precursor preparations were ordered from Xi'an p-OLED (China), containing FAI, CsI, MABr, 4F-PEAI, PbI_2 and $PbBr_2$. The solvents of DMF, DMSO, IPA, hydrogen peroxide (H_2O_2, 30% in water), chlorobenzene (CB) and anhydrous ethanol (Et-OH) as well as the RbI were purchased from Sigma. The [2-(3,6-Dimethyl-9H-carbazol-9-yl)butyl]phosphonic acid (MeO-2PACz) , BCP and 1,3-Propanediammonium Iodide ($PDAI_2$) were bought from TCI company. The C_{60} powders were offered by J&K Scientific. The perovskite precursors (1.5 M) were prepared according to the literature[1] and additionally adding 4F-PEAI (0.6 mg/mL). The MeO-2PACz powders were dissolving in the Et-OH with concentration of 0.5 mg/mL, and the solutions should be ultrasonically treated for 5 minutes to break the clusters before using. The $PDAI_2$ was dissolved in IPA (0.3 mg/mL) as surface passivation.

Solar cells fabrications

The FTO substrates were ultrasonically cleaned in detergent, deionized water, acetone, and IPA for 15 min. After dried under N_2 flow, the FTO substrates were further cleaned with UV ozone for 15 min. To seed the -OH groups on the FTO, the FTO substrates were bathed into H_2O_2 solution with concentration of 10% (in DI water) in the Petri dish, and then exposed to UV treatment for 5 min. After that, the clean substrates were transferred into glovebox with N_2 as protection gas to coat SAMs, perovskite and passivation layers, sequentially. The coating procedures of perovskite is two steps: low speed at 1000 rpm (accelerated speed of 1000) for 10 s and then 4000 rpm (accelerated speed of 2000) for 40 s. 150 μL CB as antisolvent was treated on the wet film at the 10 s before the end. The substrates were annealed at 100 °C for 15 min to transmit the intermediate phase into photovoltaic phase. $PDAI_2$ surface treatments (0.3 mg/mL in IPA) were conducted on the cool perovskite films at 4500 rpm for 30 s with the dynamic coating, and then annealed at 100 °C for 5 min. The substrates were transferred into vacuum chamber to thermally evaporate 25 nm C_{60}, 6 nm BCP and 120 nm Ag

respectively. After all procedures, 150 nm LiF was evaporated on the glass side as the anti-reflection layers before J-V data collections. For room and high-temperature MPPT, the BCP and Ag electrodes were replaced by 25 nm ALD-SnO_2 and 100 nm Au, respectively. The active areas of the solar cells were defined by the overlapping area of top electrodes and bottom FTO. The mini-modules were fabricated as the same procedures as the unit cells on the 5×5 cm^2 FTO substrates and 350 μL CB was used as antisolvent. The P1, P2 and P3 lines were scribbled with the green laser and the controlled geographic fill factor was 94.5%.

Characteristics

The *J-V* curves were collected with the Keithley 2400 sourcemeter under solar simulator (AM 1.5, Enlitech, SS-F5-3A). The spectrum of the simulator was calibrated with the standard Si solar cell (Enli/SRC2020, SRC-00201). The EQE spectra of the devices were measured on the model IVQE8-C. The XPS measurements of the FTO and FTO/SAMs were obtained from Kratos AXIS ULTRA, where the data were fitted on the Casa XPS with the fixed FWHM values.[2] The AFM and KPFM images of the films were performed on the Dimension 3100. The modes for KPFM measurements were defined as sample surface minus tips. The crystallinity of the perovskite films was investigated by X-ray diffraction (XRD, Bruker AXS D8 Advances Germany) and scanning electronic microscope (SEM, Zeiss GeminiSEM450). The statistics results of grain size were obtained by the commonly used Nano Measurer, where we took all the grains into account. The GIXRD patterns of the films were collected on Rigaku Smartlab with the incident angle of 1°. PL and PL mappings of perovskite films were measured at the Renishaw inVia Reflex with excited light of 532 nm laser. The TRPL curves were obtained at Horiba Scientific Cm., Japan. The TPC, TPV and MS curves were recorded with the electrochemical workstation (Solartorn 1260A impedance analyzer). The DFT calculations were conducted according to the previous literatures with similar parameters.[3,4]

Stability measurements

The hyperspectral PL images of the perovskite were conducted on Renishaw inVia

Reflex with the 532 nm laser illumination. The intensity of the laser is equal to 1 sun (100 mW/cm^2). The illumination direction was from glass to perovskite to identify the perovskite/SAMs/FTO interface. The room-temperature and high-temperature MPPT was measured on the temperature-controlled oven and the intensity of the white LED was around 1 sun. All devices and films for stability measurements were encapsulated by UV epoxy with the covered glass. For better contact for high-temperature MPPT test, the indium was covered on Au electrode. All measurements were conducted in the ambient condition with RH>40%.

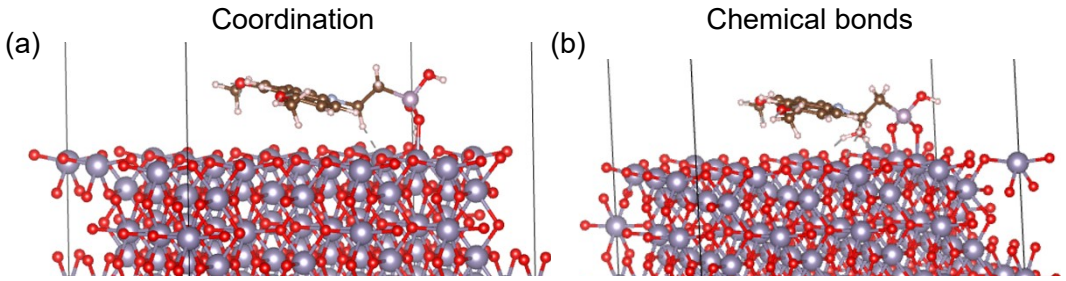

Fig. S1. Schematic illustrations of the binding types when depositing SAMs on TCO based on theoretic simulations.

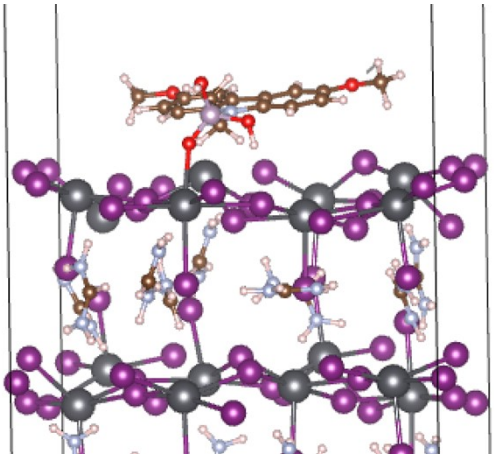

Fig. S2. Schematic illustrations of SAMs coordinating on $FAPbI_3$ with Pb-I termination.

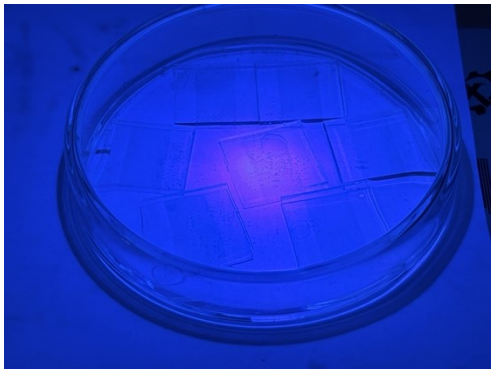

Fig. S3. Photo of the FTO bathing into H_2O_2/UV treatment for seeding -OH groups.

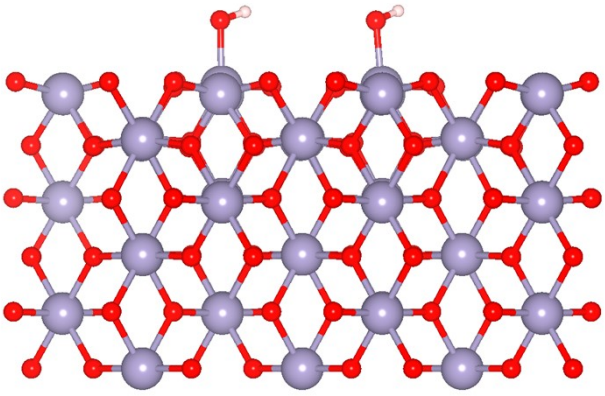

Fig. S4. Schematic diagram of the OH radicles absorbing on FTO substrates from DFT simulations.

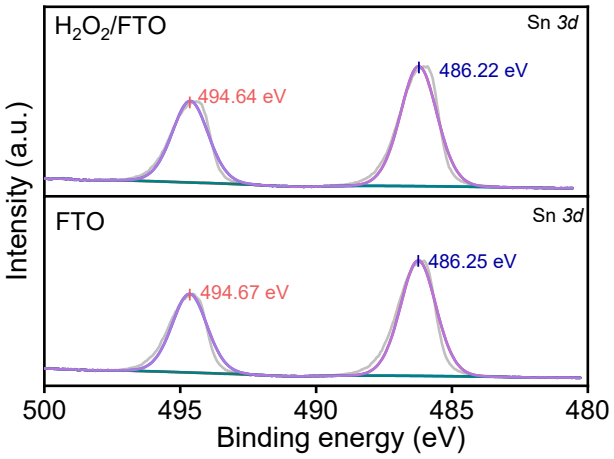

Fig. S5. Sn 4f XPS spectra of the FTO with and without H_2O_2/UV treatment.

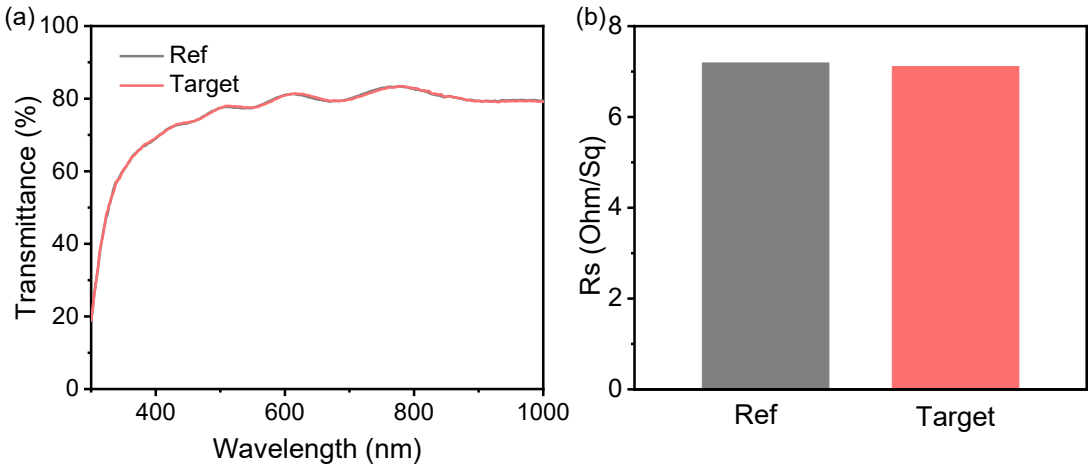

Fig. S6. Transmittance curves and square resistivity of FTO with and without H_2O_2/UV treatment.

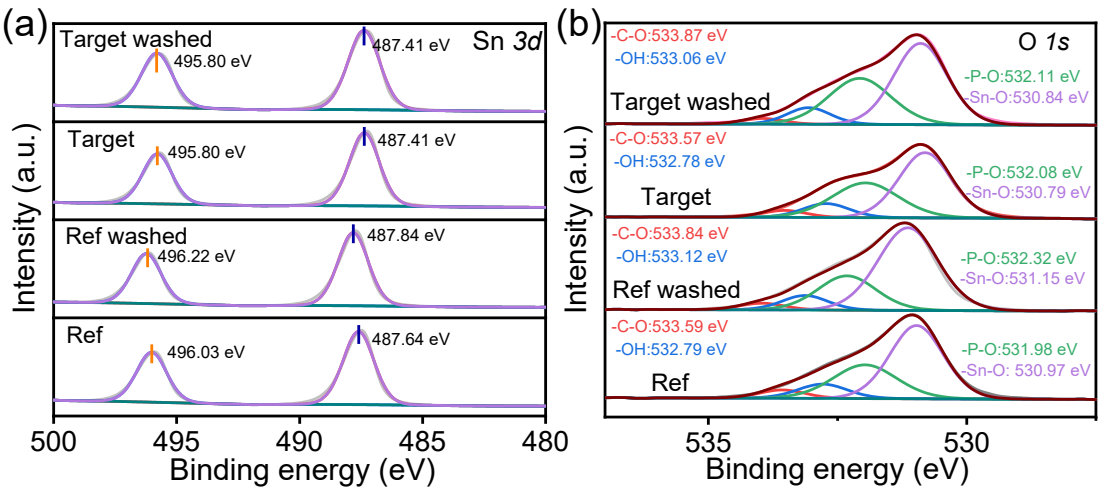

Fig. S7. Sn *3d* (a) and O *1s* (b) XPS spectra of the SAMs covered FTO with and without H_2O_2/UV treatment before and after DMF washing. The Ref samples show the chemical shift toward larger binding energy of both -Sn-O and -P-O signals after DMF washing, corresponding to the delamination of fragile coordination. Whereas seeding -OH groups cure the SAMs adsorption on FTO and slight shifts can be detected after same treatment.

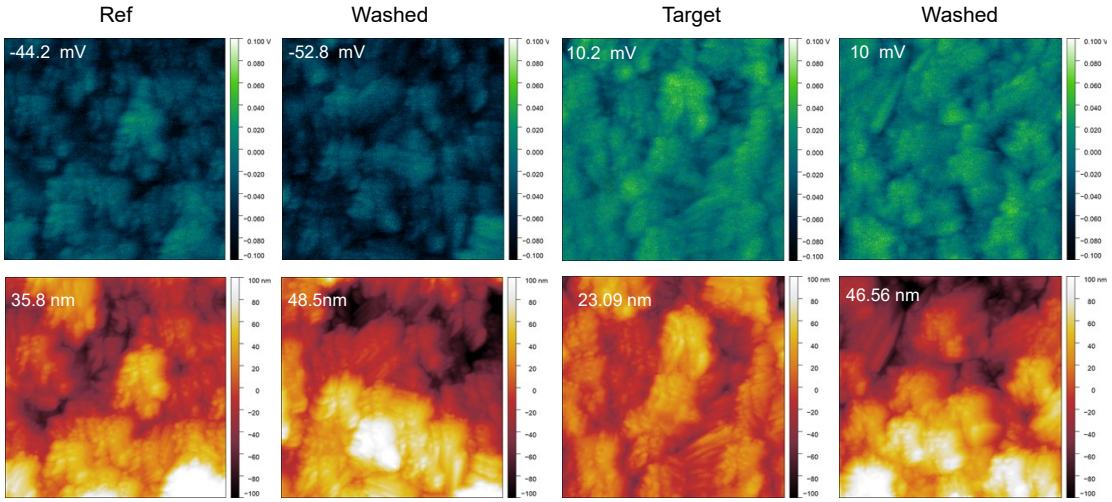

Fig. S8. The KPFM (top panel) and AFM images of the SAMs covered FTO substrates before and after DMF washed.

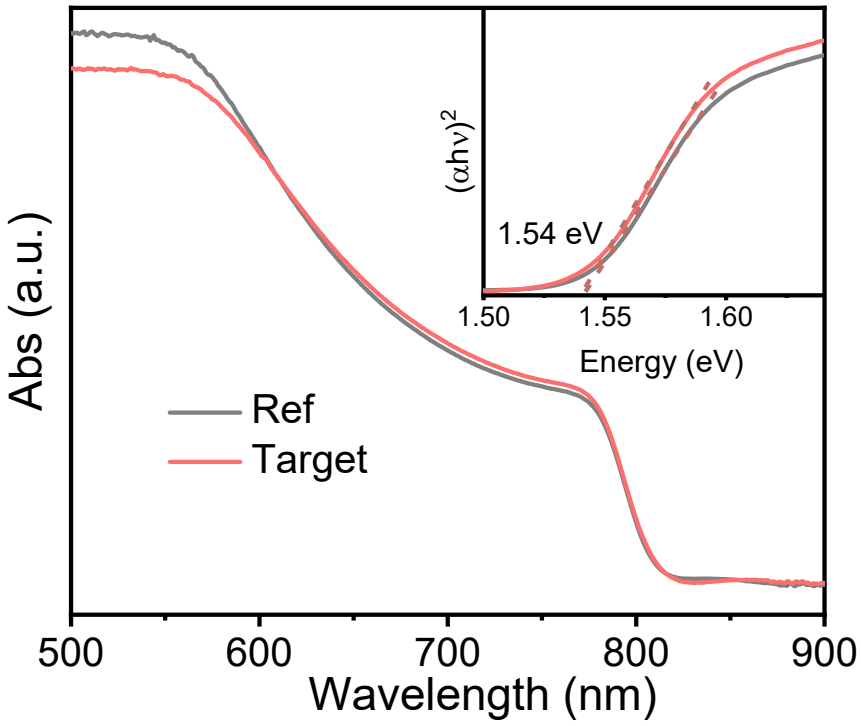

Fig. S9. UV-vis absorption spectra of the Ref and Target perovskite films. The inset figure is the fitted Kubelka-Munk spectra.

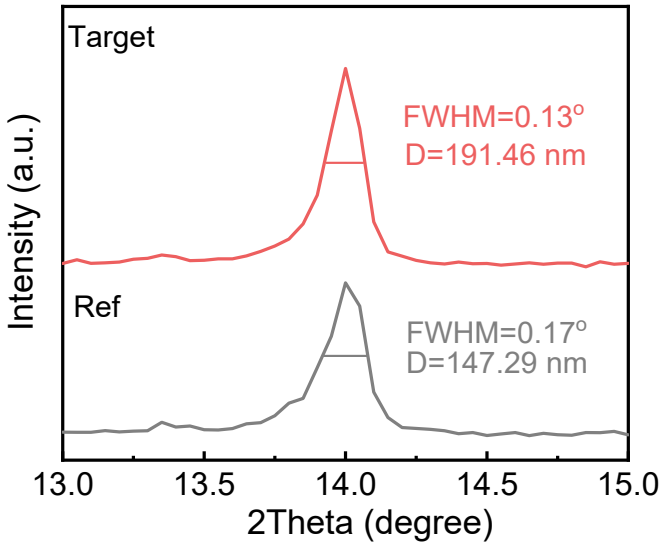

Fig. S10. Grain sizes fitted from XRD patterns based on the Debye-Scherrer equation.

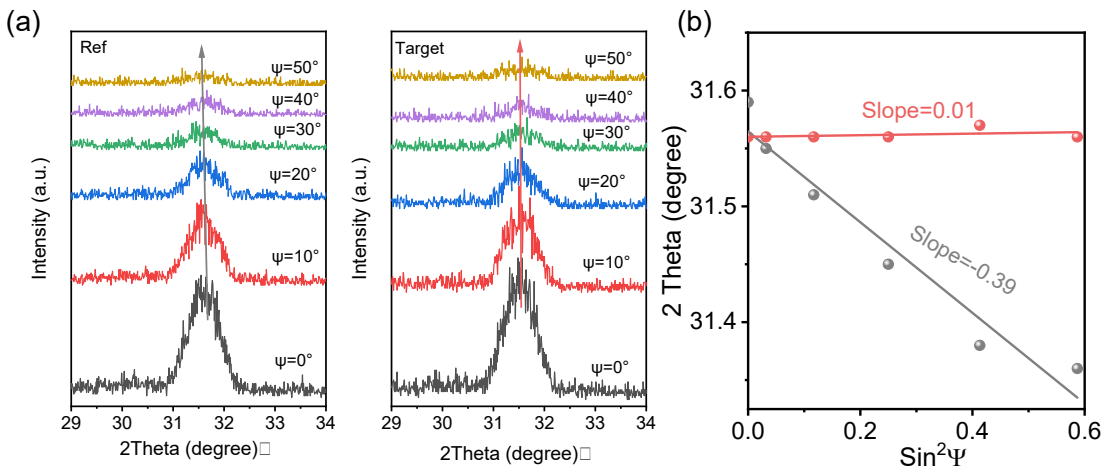

Fig. S11. GIXRD patterns (a) at different Ψ angles and the linear fit relationship of 2theta-sin^2(Ψ).

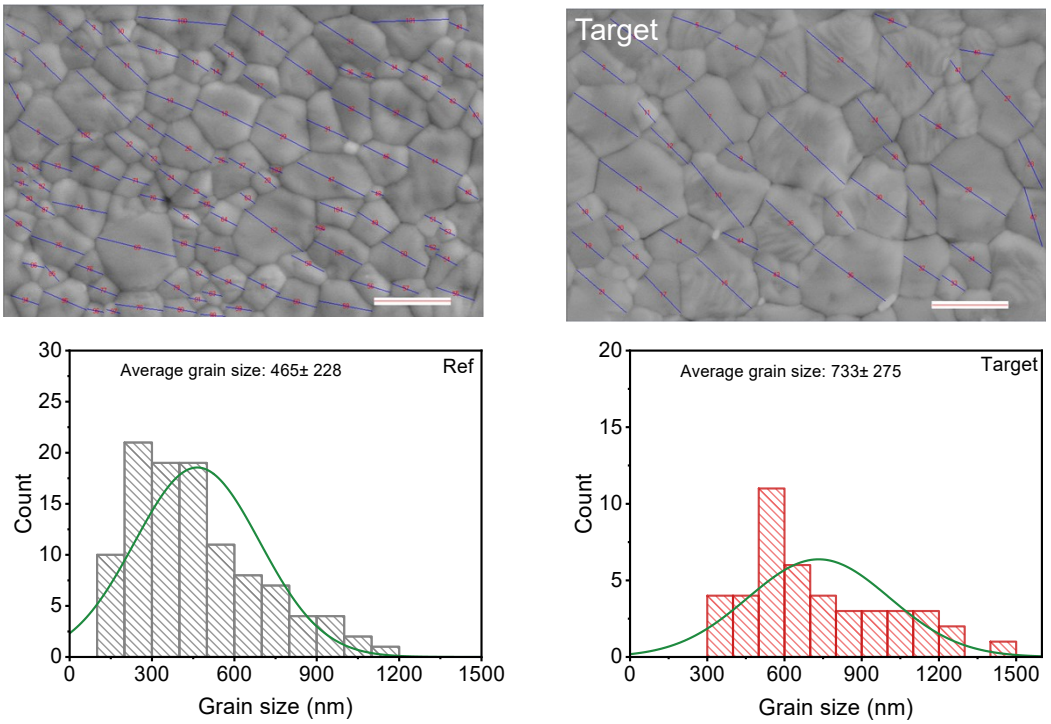

Fig. S12. Grain size statistics results based on the SEM images.

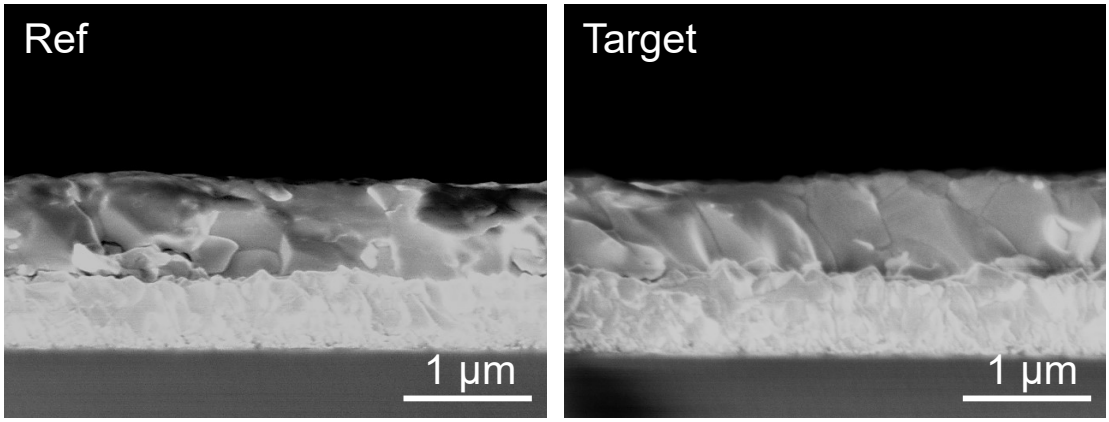

Fig. S13. Cross-section SEM images of the Ref (left) and Target (right) perovskite films.

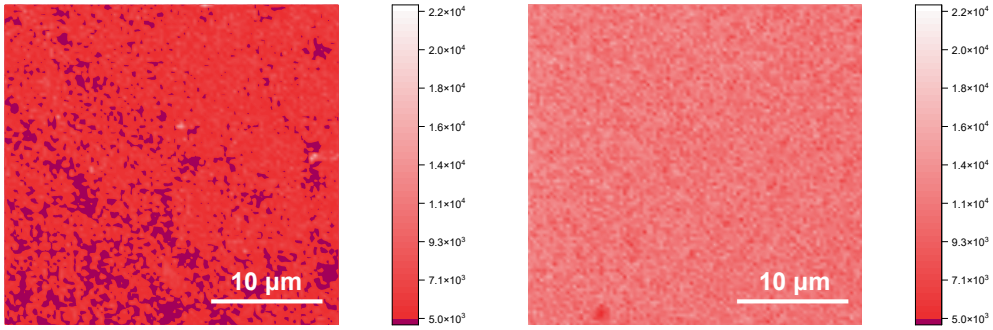

Fig. S14. PL mappings of the Ref (left) and Target (right) perovskite films.

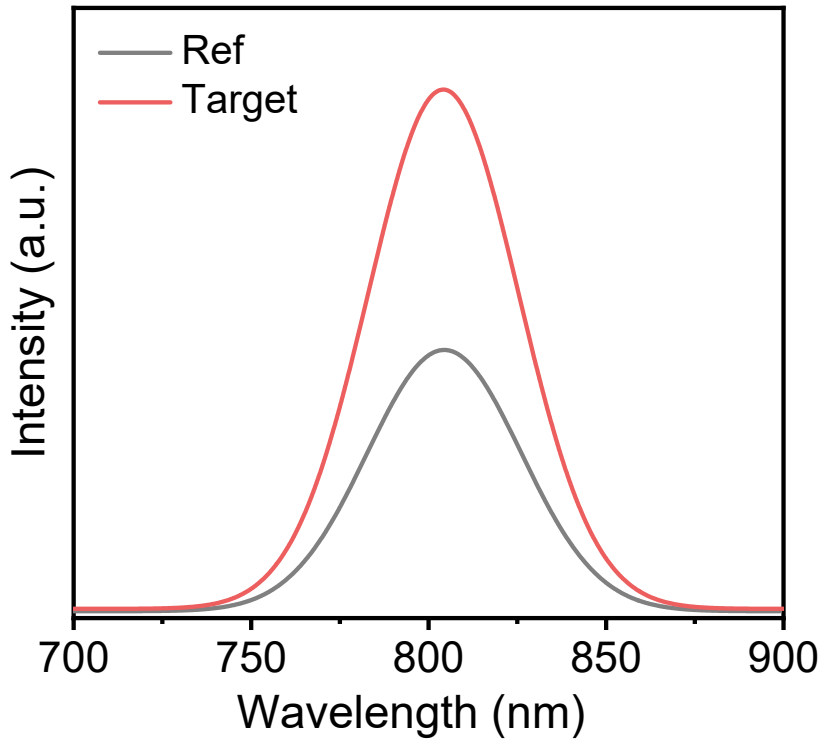

Fig. S15. PL curves of the Ref and Target perovskite films.

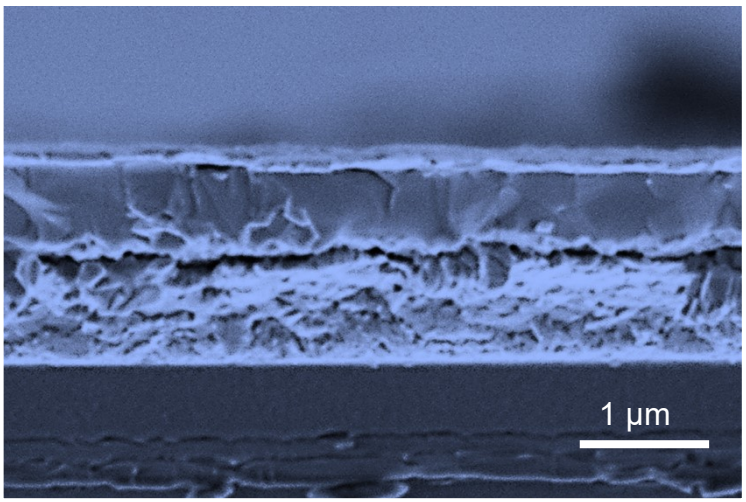

Fig. S16. Cross-section SEM image of the PSCs.

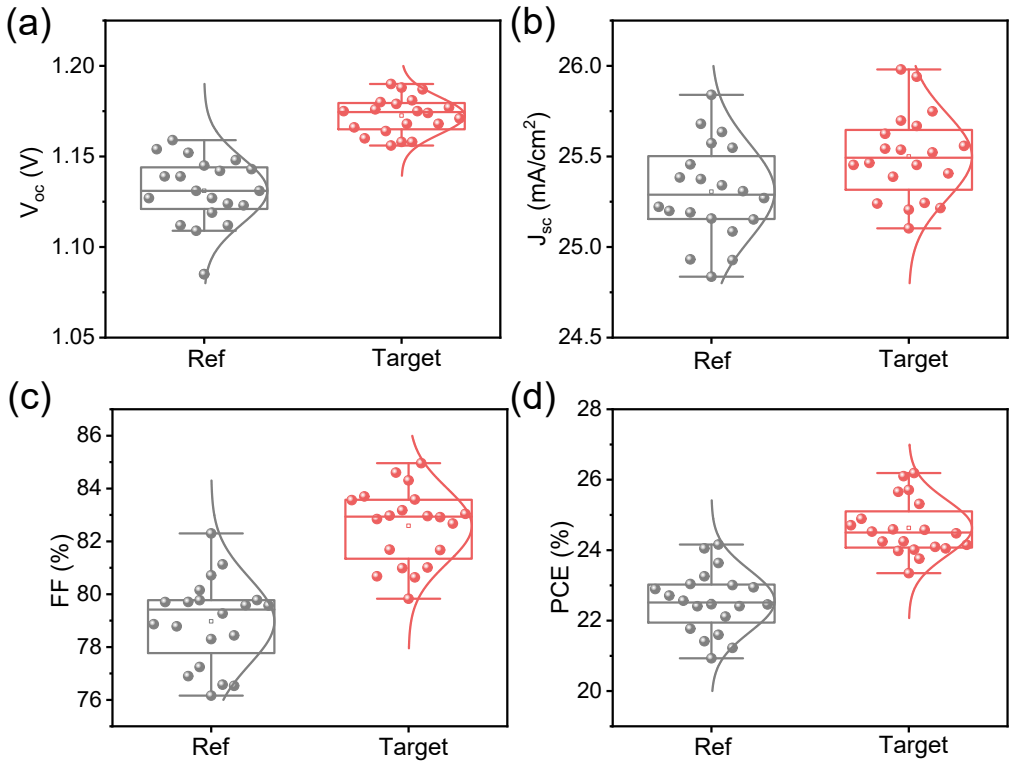

Fig. S17. Statistics photovoltaic parameters of the Ref and Target devices.

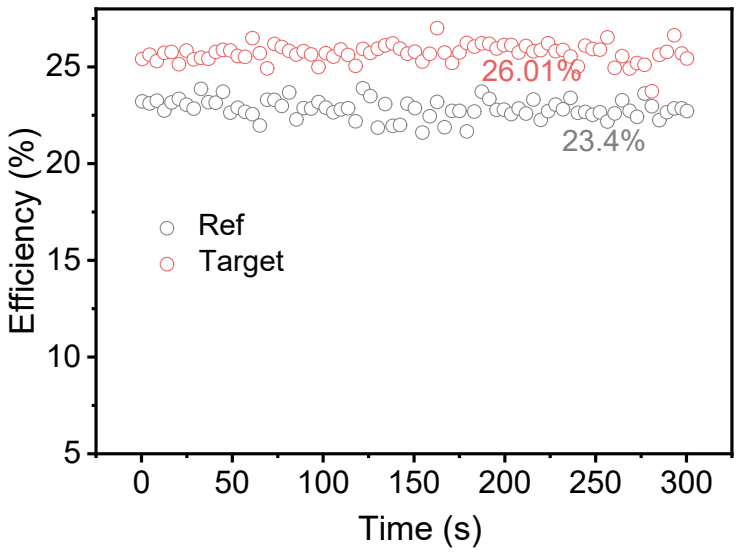

Fig. S18. SPO curves of the champion device of Ref and Target.

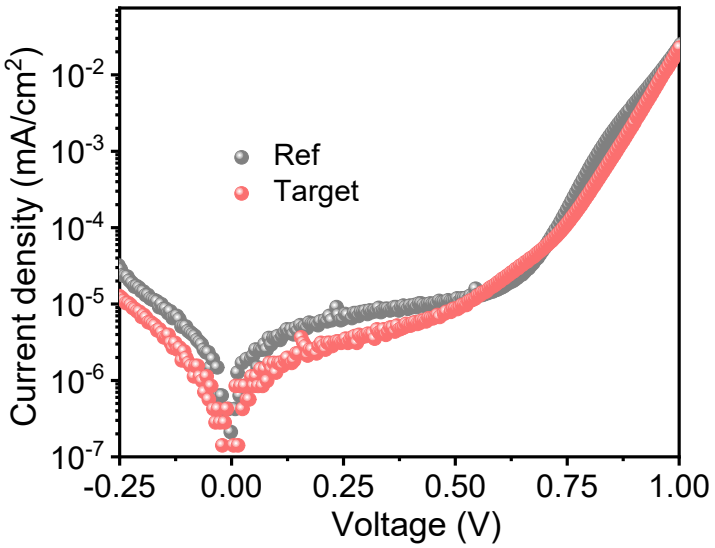

Fig. S19. Dark J-V curves of the ref and target devices.

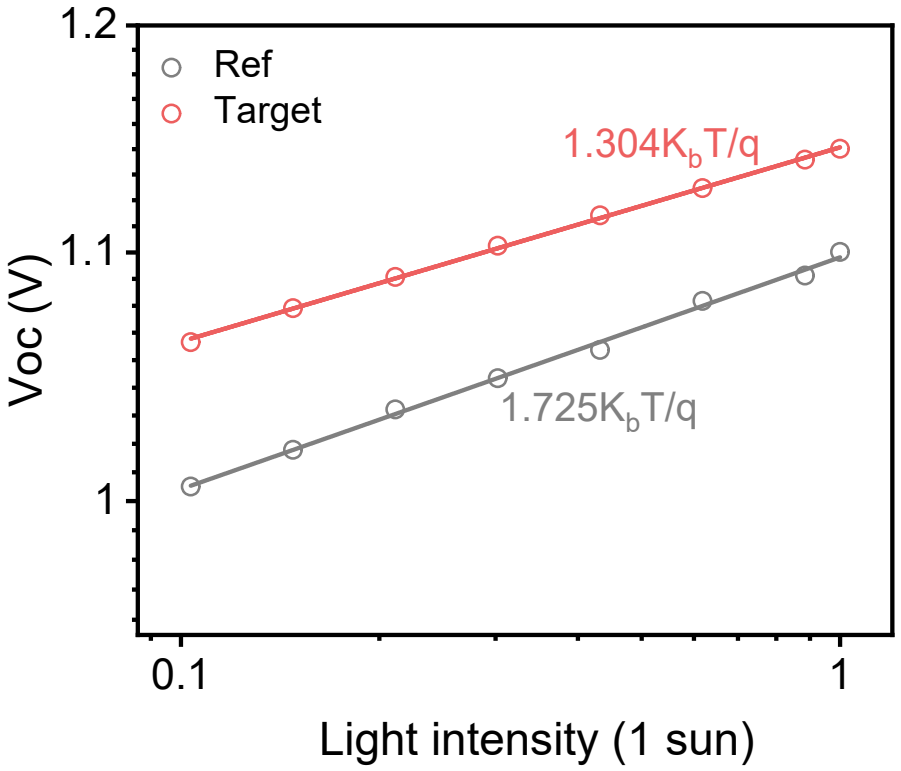

Fig. S20. The V_{OC}-light intensity dependence measurements, and the n values are fitted based on the literatures.

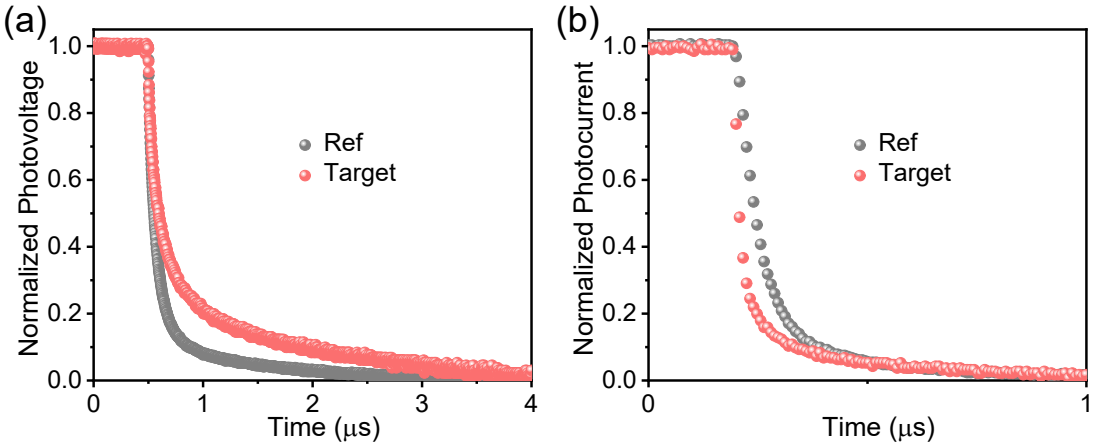

Fig. S21. TPV and TPC curves of the Ref and Target PSCs.

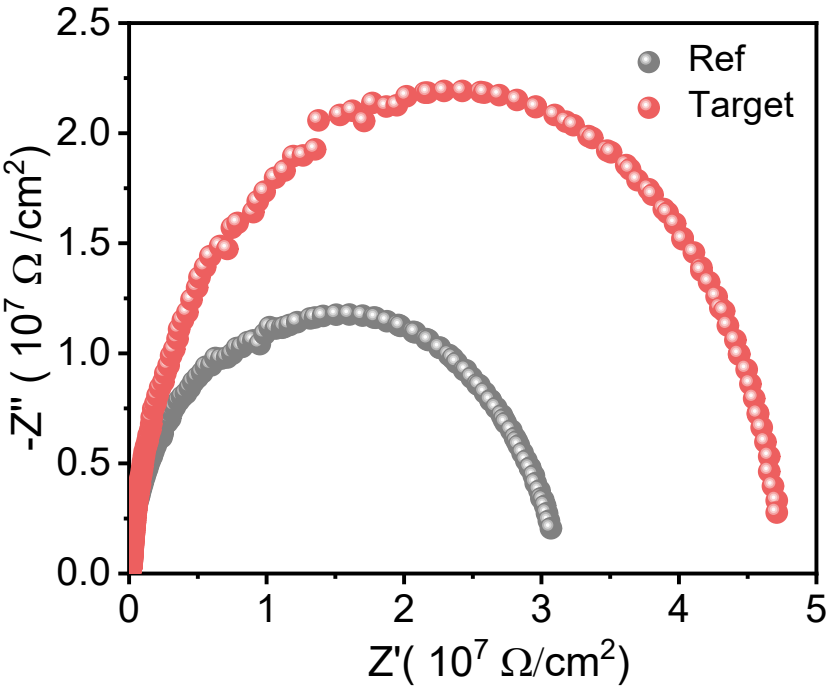

Fig. S22. Nyquist plots of the Ref and Target PSCs.

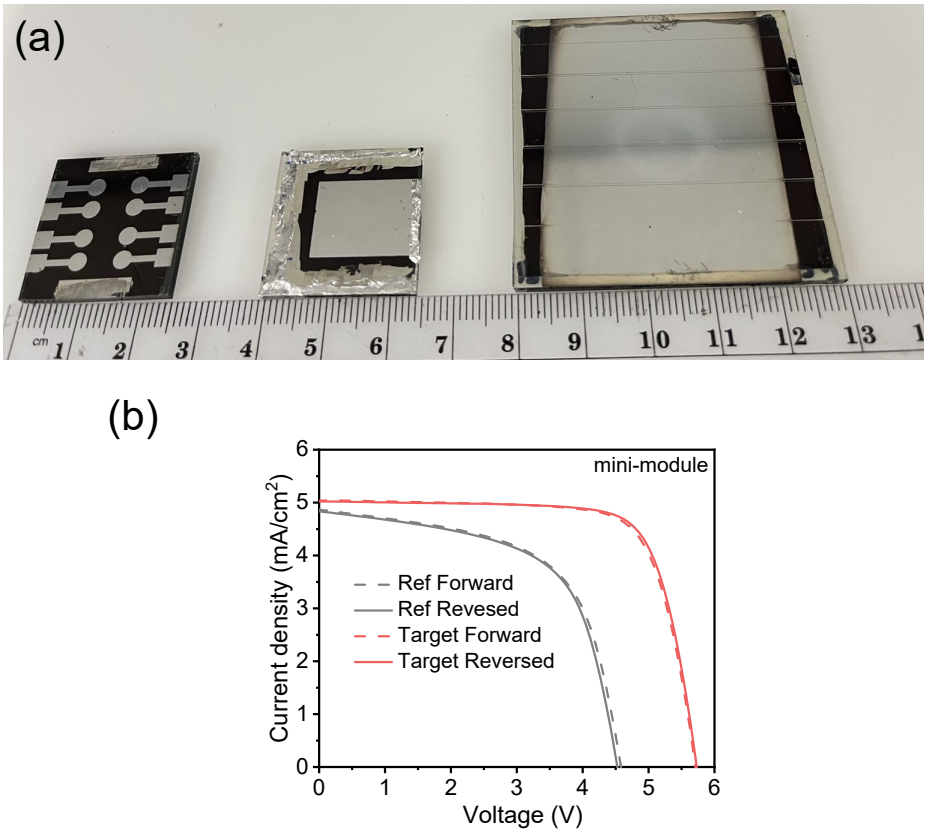

Fig. S23. a) Photo of the unit cell (left, with area of 0.071 cm^2), large-area device (medium, 1.21 cm^2) and mini-module (right, 14.64 cm^2). b) J-V curves (active area) of

the minimodules.

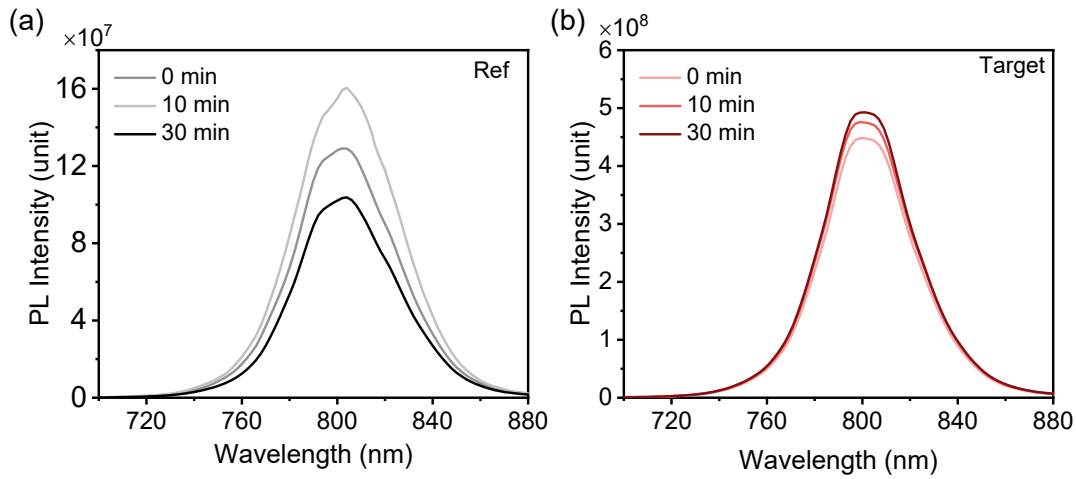

Fig. S24. The PL curves of the Ref (a) and Target (b) perovskite films during the micro-PL ages for different time.

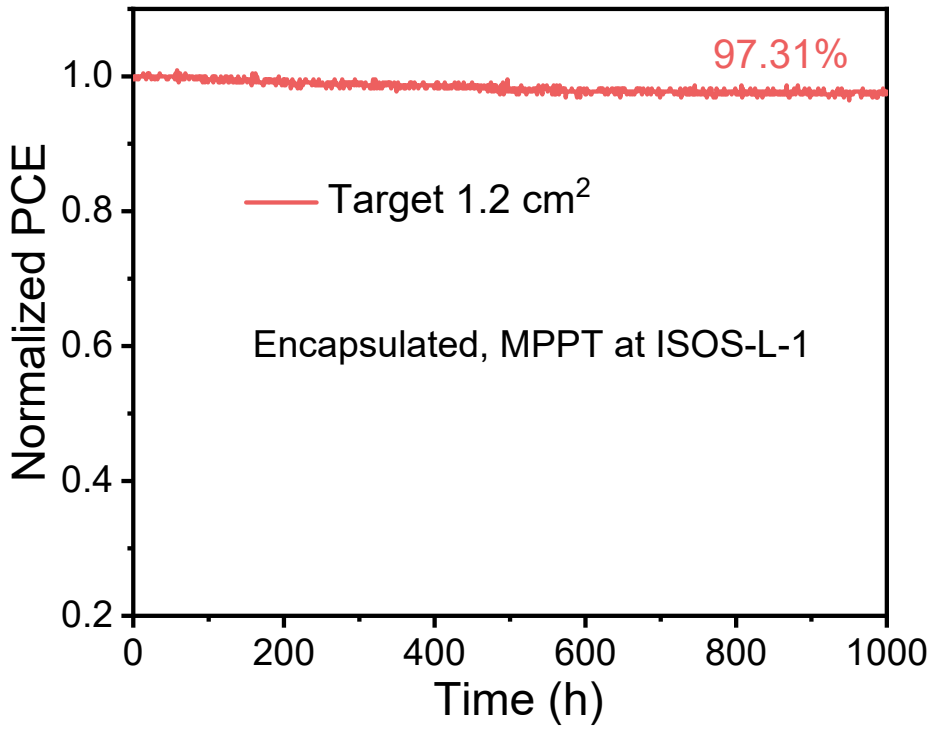

Fig. S25. MPPT of Target devices under ISOS-L-1 test.

Table S1. Fitting results of the TRPL curves.

Samples	A_1	τ_1/ns	A_2	τ_2/ns	τ_{avg}/ns
Ref	0.59	48.8	0.41	302	152.6
Target	0.48	179	0.52	540	366.7

Table S2. Photovoltaic parameters of the devices.

Samples	V_{OC}/V	J_{SC}/mA/cm^2	FF/%	PCE/%
Ref F	1.137	25.62	77.08	22.45
R	1.152	25.62	81.87	24.16
	1.131±0.018	25.31±0.26	78.97±1.64	22.55±0.88
Target F	1.185	25.96	84.32	25.94
R	1.188	25.95	84.96	26.19
	1.173±0.01	25.49±0.24	82.59±1.4216	24.63±0.78
1.21 Ref F	1.113	24.06	70.94	18.99
R	1.109	23.98	70.43	18.73
1.21 Target F	1.185	25.65	81.20	24.68
R	1.186	25.64	81.13	24.67
Ref Module F	4.582	4.86	59.68	13.29
R	4.527	4.84	60.28	13.20
Target Module F	5.712	5.04	74.46	21.44
R	5.732	5.03	75.51	21.77

References

1. Q. Jiang, J. Tong, Y. Xian, R. A. Kerner, S. P. Dunfield, C. Xiao, R. A. Scheidt, D. Kuciauskas, X. Wang, M. P. Hautzinger, R. Tirawat, M. C. Beard, D. P. Fenning, J. J. Berry, B. W. Larson, Y. Yan, K. Zhu, *Nature* 2022, **611**, 278-283.

2. G. H. Major, N. Fairley, P. M. A. Sherwood, M. R. Linford, J. Terry, V. Fernandez and K. Artyushkova, *J. Vac. Sci. Techn. A*, 2020, **38**.

3. K. Zhao, Q. Liu, L. Yao, C. Deger, J. Shen, X. Zhang, P. Shi, Y. Tian, Y. Luo, J. Xu, J. Zhou, D. Jin, S. Wang, W. Fan, S. Zhang, S. Chu, X. Wang, L. Tian, R. Liu, L. Zhang, I. Yavuz, H. F. Wang, D. Yang, R. Wang, J. Xue, *Nature* 2024, **632**, 301-306.

4. Z. Li, X. Sun, X. Zheng, B. Li, D. Gao, S. Zhang, X. Wu, S. Li, J. Gong, J. M. Luther, Z. Li, Z. Zhu, *Science* 2023, **382**, 284-289.